

Pb substitution in the $\text{Bi}_2\text{Sr}_2\text{CaCu}_2\text{O}_{8+\delta}$ high- T_c superconductor: Cation overdoping

C. Kendziora, S. B. Qadri, and E. Skelton
Naval Research Laboratory, Washington, DC 20375
 (Received 27 May 1997)

We study the effects of Pb substitution in single crystals of the high-temperature superconductor $\text{Bi}_2\text{Sr}_2\text{CaCu}_2\text{O}_{8+\delta}$. We compare Pb-substituted samples with ‘‘pure’’ (unsubstituted) crystals in terms of structure, cation composition, and the temperature dependences of ac susceptibility and Raman scattering. We find that Pb^{2+} primarily substitutes for Bi^{3+} , leading directly to a T_c reduction characteristic of overdoped samples. We also observe structural changes related to the superlattice modulation along b^* . Raman scattering studies indicate that some Pb atoms go to Sr sites. Low-temperature electronic Raman scattering shows further evidence for cation overdoping by comparison with oxygen annealed pure $\text{Bi}_2\text{Sr}_2\text{CaCu}_2\text{O}_{8+\delta}$.
 [S0163-1829(97)03246-3]

Among the most interesting and potentially instructive aspects of the high-temperature superconducting cuprates is their high sensitivity of T_c to doping level. Recent experiments in the underdoped superconductor regime (where T_c increases with increased carrier concentration) have yielded great insight into the unique properties of the cuprates. The overdoped regime may prove equally critical to our understanding of the mechanism of superconductivity in this class of materials.

In the particular superconductor $\text{Bi}_2\text{Sr}_2\text{CaCu}_2\text{O}_{8+\delta}$ (Bi2212), with a maximum T_c of ≈ 90 K, both cation substitution and postannealing in low oxygen partial pressures offer access to the entire underdoped regime with only minimal changes to the crystal structure. The substitution of Y^{3+} or rare-earth elements¹ at the Ca^{2+} site provides a mechanism to lower the carrier concentration throughout the underdoped regime and into the antiferromagnetic insulating phase. Similarly, annealing as-grown crystals in a reduced oxygen atmosphere can place them down the doping curve as far as the insulator range.² In contrast, the means for accessing the overdoped region have not proven as effective in Bi2212 as they have in $\text{Tl}_2\text{Ba}_2\text{CuO}_{6+\delta}$ (Tl2201) (Ref. 3) or $\text{La}_{2-x}\text{Sr}_x\text{CuO}_{4+\delta}$ (La214),⁴ where the ‘‘normal metal phase’’ can be observed.

Annealing Bi2212 in high-pressure oxygen has been observed to lower T_c to ~ 50 K on the *overdoped* side.² In terms of the superconducting energy gap, this degree of overdoping is enough to observe symmetry-independent 2Δ peaks in the electronic Raman continuum^{5,6} (perhaps indicative of an isotropic order parameter) and a pronounced reduction in the size of the gap relative to T_c ($2\Delta/k_B T_c \approx 5$). However, it is not far enough to approach the weak-coupling BCS limit ($2\Delta/k_B T_c = 3.52$), as is seen in Tl2201.^{5,7} The primary *cationic* substitution that leads to a larger hole carrier concentration in Bi2212 is the exchange of Pb^{2+} for Bi^{3+} in the weakly bonded BiO_2 layers.⁸⁻¹¹ In this work, we study the effects of such a substitution on the composition and structure of the Pb-doped crystals. We also study the temperature dependences of ac susceptibility and the polarization-dependent Raman scattering spectrum for Pb-doped crystals and compare these with properties of the pure Bi2212 compound.

I. GROWTH AND PREPARATION

Each of the crystal growth preparations used identical stoichiometric ratios ($[\text{Bi}]+[\text{Pb}]:[\text{Sr}]:[\text{Ca}]:[\text{Cu}]=2:2:1:2$) of cations. The Pb substituted samples each had a nominal Pb content $[[\text{Pb}]/([\text{Pb}]+[\text{Bi}])]$ of 20%, corresponding to $\text{Bi}_{1.6}\text{Pb}_{0.4}$ in the customary formula units. Each of the batches were grown by heating the premixed unreacted oxide and carbonate powders to 1000 °C and cooling at the rate of 1.5 °C/hour to 700 °C, at which point the crucible was quenched to room temperature. Upon breaking the crucible, shiny micaceous flakes with typical dimensions of a few mm on a side and tens of microns in thickness were mechanically cleaved from the surrounding solid flux.

Subsequent postanneals of individual crystals were carried out at temperatures ranging from 450 to 550 °C in three different ways. Ambient atmosphere anneals were performed with open air circulation. Low-pressure oxygen anneals were conducted in sealed quartz tubes at various oxygen partial pressures. Oxygen anneals were carried out in cells capable of withstanding pressures in excess of 0.2 GPa.

II. COMPOSITION

Figure 1 shows the energy dispersive x-ray spectrum (EDX) of Bi2212 single crystals measured with 25 KeV electrons in a scanning electron microscope. The thick dashed curve represents data from a pure sample, while the thin solid line plots the EDX spectrum of a Pb-substituted crystal under identical conditions. As is clearly shown in the figure, the displayed energy range contains characteristic fluorescence x rays for each of the cations. The substitution of Pb is readily discerned by observing the intensity of the L lines in the range of 10–14 KeV (inset). Attempts to measure the oxygen concentrations with EDX proved irreproducible and are therefore not discussed. Instead, each of the crystals studied had been postannealed under the same conditions (500 °C in air atmosphere), in the hope of achieving uniformity in oxygen content.

A detailed analysis of the characteristic x-ray intensities for several crystals from different growth batches yields the cation compositions shown in Table I. The numerical analy-

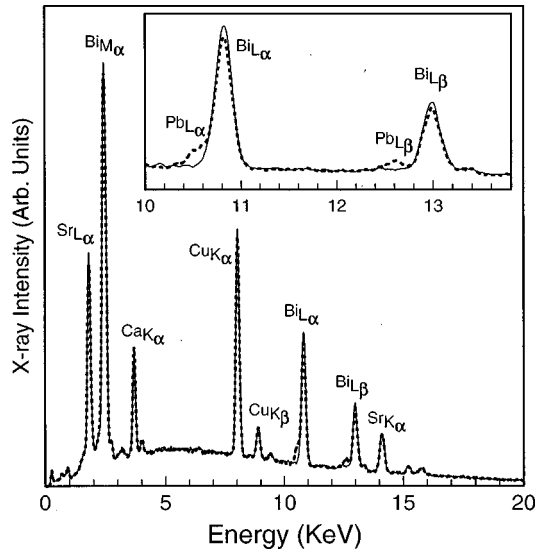


FIG. 1. The energy dispersive x-ray (EDX) spectrum of Bi2212 single crystals measured with 25 KeV electrons. The solid curve represents data from a pure (Pb-free) sample, while the dashed line plots the EDX spectrum of a Pb-substituted crystal under identical conditions. (Inset) The substitution of Pb is readily discerned by observing the intensity of the L lines in the range of 10–14 KeV.

sis technique employed integrates the x-ray peaks and accounts for matrixing effects of the presence of one element on the observed concentration of another. It relies on the use of a standard, chosen here to be a pure Bi2212 crystal. The resulting values may have systematic deviations due to the uncertainty of the standard, but are useful for direct comparisons of the crystals studied. For straightforward comparison, the compositions of each sample are normalized to $[Cu]=2$, where $[]$ denotes the concentration of a given element. The observation that the sum of the other cations remains fairly constant from sample to sample is an indication of consistency in the Cu concentration.

Several results of the compositional analysis become evident upon inspection of the data in Table I. First, since there is uncrystallized material remaining in the crucible, the concentrations measured in each crystal do not necessarily correspond to the nominal values. Nonetheless, we note that $[Pb]+[Bi]$ is roughly constant across all samples, suggesting

that Pb does go primarily to the Bi site. Second, T_c of the Pb crystals decreases relative to the pure samples, presumably due to overdoping.

However, the direct correlation of Pb content with T_c may be obscured by variability in the Sr/Ca ratio. In their study of Sr/Ca ratio in Bi2212, Sekine *et al.*¹² observed that excess Ca on the Sr site reduces T_c for samples with low oxygen content, while retaining a similar low T_c for those with high oxygen content. This raises the question of the degree to which the effects observed in our samples are due to Pb substitution or the observed shift in Sr/Ca ratio. Because it is possible to raise the T_c of Pb substituted samples with similar Sr/Ca ratio to ours as high as 90 K with an anneal in Ar,¹⁰ the results of Sekine *et al.* (indicating the annealing insensitivity of T_c upon Ca substitution at the Sr site) indicate that the drop in T_c is due to overdoping associated with Pb substitution.

III. STRUCTURE

The a - b plane structure of the sample was studied with high-resolution transmission electron microscopy (TEM). Single crystals were cleaved until transparently thin ($t \approx 1000$ Å) and mounted on copper TEM grids. Electrons of 300 keV were used to generate images of the surface as well as (001) diffraction patterns. The spot size of the electron beam was on the order of 1 μ m.

Figure 2 is an image of the a - b plane surface of a Pb-substituted Bi2212 crystal. The magnification factor for the film was 500 000X. The directions of a and b are shown in the figure. Dark fringes attributed to the superlattice modulation in b are visible running along the a -axis direction. Measurements of the small squares, each representing a unit cell, yield approximate values for the a and b lattice parameters ($a \approx b \approx 5.4$ Å) which agree with previous results^{8,10,11} within the experimental uncertainty. The lighter (right) portion of the figure represents an area off the edge of the crystal. At the sample edge, an amorphous (presumably carbonaceous) region is observed, most likely due to a residue of the glues and solvents used in the preparation process.

Figure 3 shows an (001) diffraction pattern measured from an area adjacent to that in Fig. 2. The overall pattern is similar to that seen in pure Bi2212 (Refs. 1,10) with several

TABLE I. The results of EDX compositional and x-ray structural analysis of pure and Pb-substituted Bi2212 single crystals. Pb 1 and Pb 2 refer to the different Pb-substituted batches. A and B refer to different crystals from the same growth batch.

Sample	T_c (K) ^a	[Bi]	[Pb]	[Sr]	[Ca]	[Cu] ^b	%Pb ^c	Sr/Ca	a (Å)	b (Å)	c (Å)
Standard	84	2	0	2	1	2	0	2			
Pure #2	84	2.05	0	1.99	0.94	2	0	2.12	5.410	5.412	30.928
Pb 1 A	80	1.85	0.19	1.90	1.17	2	9.3	1.62	5.401	5.410	30.743
Pb 1 B	80	1.82	0.19	1.96	1.18	2	9.5	1.66			
Pb 2 A	75	1.84	0.17	1.94	1.06	2	8.5	1.83	5.386	5.419	30.806
Pb 2 B	75	1.84	0.15	1.89	1.07	2	7.5	1.77			

^a T_c when annealed in air at 500 °C.

^bEach sample normalized to $[Cu] = 2$.

^c%Pb is defined as $[[Pb]/([Pb]+[Bi]) \times 100$.



FIG. 2. A high-resolution TEM image of the a - b plane surface of a Pb-substituted Bi2212 crystal.

new features of interest apparently unique to the Pb-substituted structure. Primarily, the superlattice modulation (right arrow) is observed along b^* , corresponding to a wavelength of $6.8b$, in general agreement with earlier results for samples with similar Pb concentrations.^{8,11} This is considerably longer than the superlattice length in pure Bi2212

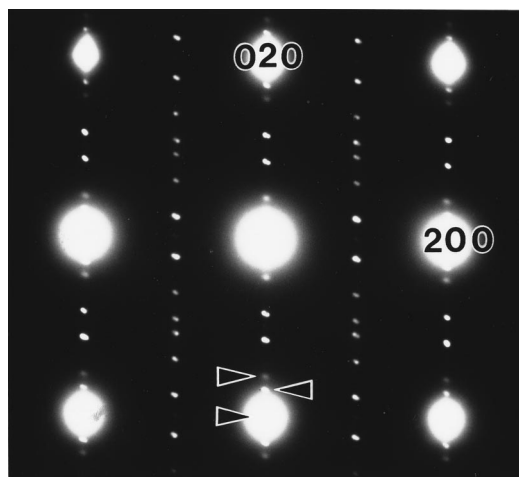


FIG. 3. An (001) TEM diffraction pattern from a thin Pb-substituted Bi2212 single crystal.

(4.7*b*), a relaxation which suggests a better lattice matching between the stacked BiO_2 and CuO_2 layers. However, a second faint superlattice spot (top left arrow) can be observed at each $(n, n+0.22, 0)$, where n is every even integer. This indicates that there is some remnant of the “pure” modulation, even at this level of Pb substitution.⁸ Upon close inspection of the high-resolution image (Fig. 2), the dark fringes along the a direction do not maintain an equidistant spacing. Instead, they appear to toggle back and forth, a visual manifestation of the local variations in the superlattice modulation.

The in-plane structure remains quite asymmetric and there is no evidence for an orthorhombic-to-tetragonal structural phase transition with Pb substitution. More precise measurements of the a and b lattice constants from magnified diffraction images further indicate orthorhombicity with $a=5.46(1)$ Å while $b=5.52(1)$ Å. Although these values may be systematically large due to an uncertainty in the image magnification, they are useful for comparison and follow the trends observed with the more accurate x-ray diffraction technique.

It is interesting to note that each well resolved diffraction spot in Fig. 3 appears as a doublet upon close inspection, with the angle between components roughly corresponding to the (3,1,0) direction. We do not observe the streaking of superlattice spots evident in earlier studies,^{9,10} possibly due to a somewhat lower Pb content in our crystals.

Several of the single crystals were further studied by x-ray diffraction on a four-circle goniometer to measure the a , b , and c lattice parameters. The numerical results are included in Table I. Several trends emerge when the Pb-substituted samples are compared with pure Bi2212 crystals. First, the c -axis lattice parameter decreases considerably, in analogy with oxygen overdoping.² We further observe that for the two crystals with similar Pb content, the c axis is significantly shorter in the crystal with lower Sr/Ca ratio, in good agreement with the results of Sekine *et al.*¹² The a -axis value, which is nearly equal to the b -axis value in pure Bi2212, decreases upon Pb substitution. This is in agreement with results from Pb substitution in Bi2201 crystals as well.¹³

Although the symmetry of the Pb substituted Bi2212 crystals clearly remained orthorhombic, x-ray diffraction measurements provided evidence for a - b plane twinning, which is generally not observed in the pure material. Evidence for twinning was not seen with TEM, presumably due to the smaller spot size. The x-ray-beam diameter is of the order of 1 mm, or three orders of magnitude larger than the electron beam. This would indicate that any twin grains are larger than the micron spot size of the electron beam but can be smaller than the millimeter-size x-ray beam.

In Fig. 4, we plot the x-ray scattering intensity as a function of 2θ along the nominal ($h00$) axis of a Bi2212 crystal with 8.5% Pb substitution (as measured by EDX). The strong reflection at $2\theta \approx 33^\circ$ is split into two peaks of roughly equal intensities, indicating the presence of both (200) and (020) reflections characteristic of a twinned crystal. The experimental angular resolution is smaller than the widths of the data points in Fig. 4, indicating that the peak widths are intrinsically due to a lack of long-range order (presumably in local Pb content). Simultaneous fits of these two peaks indicate a and b axis lattice parameters that are in good agree-

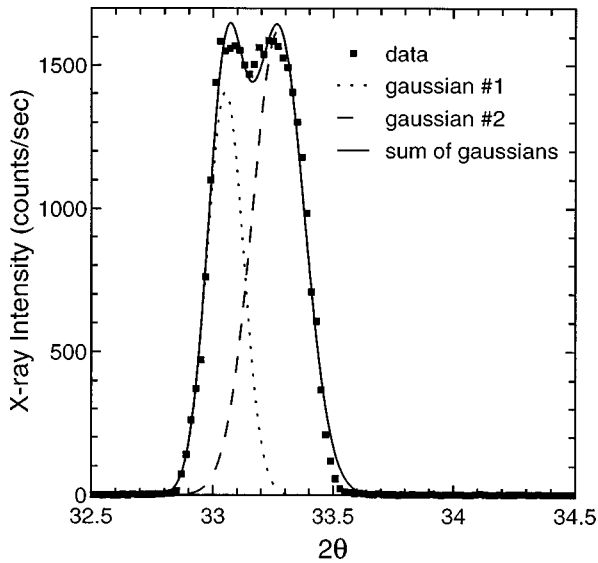


FIG. 4. The x-ray scattering intensity as a function of 2θ along the nominal $(h00)$ axis of a Bi2212 crystal with 8.5% Pb substitution (as measured by EDX). The strong scattering at $2\theta \approx 33^\circ$ is split into two peaks of roughly equal intensities, indicating the presence of both (200) and (020) reflections characteristic of a twinned crystal.

ment with other crystals. Further evidence for twinning has also been observed on this particular sample as is shown below in the section on Raman scattering. Our results confirm the observations of earlier research^{9,16} on similarly prepared samples.

IV. SUSCEPTIBILITY

ac susceptibility was used as a contactless probe of the superconducting properties of Pb-substituted Bi2212 single crystals. The results of ac susceptibility for a Pb-substituted Bi2212 crystal with different oxygen contents are plotted in Fig. 5. Such crystals exhibit a lower T_c than pure versions, as expected by doping arguments. Despite the effects of Pb substitution, the crystals appear to be underdoped when grown,

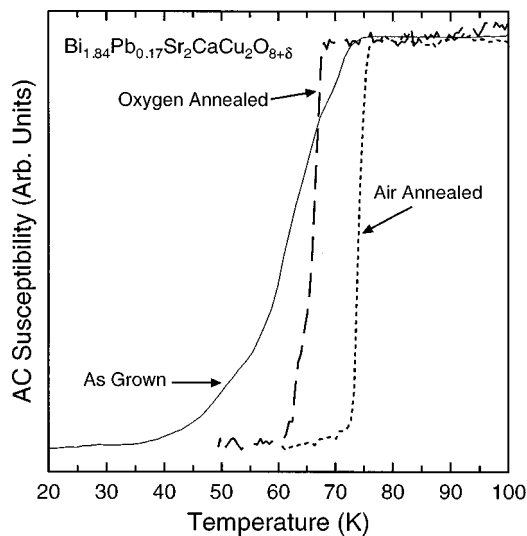


FIG. 5. ac susceptibility for a Pb-substituted Bi2212 crystal after anneals in various atmospheres.

as evidenced by the transition temperatures well below what it is possible to achieve with oxygen anneals, even in oxygen pressures >0.2 GPa. T_c increases with an anneal in air, presumably as oxygen is intercalated. The fact that T_c remains lower in Pb-substituted samples (80 K for batch 1, 75 K for batch 2) than that for similarly annealed pure Bi2212 (84 K) indicates that they are cationically overdoped. Pure Bi2212 (Ref. 14) grown by a self-flux technique similar to that used for the Pb-substituted samples, also grows underdoped, and can be tuned to a maximum T_c of 90 K with an anneal in a partial pressure of oxygen less than ambient. Fournier *et al.*¹⁰ demonstrated the same maximum T_c by Ar annealing Pb-substituted Bi2212 with a similar cation composition.

Further suggesting that the Pb-substituted crystals are overdoped is their behavior under high-pressure oxygen anneal. Anneals in high-pressure oxygen¹⁴ do not move T_c down as far as they do in pure material. There are several possible reasons for this. The first may be that the crystal resists further oxygen intercalation for structural reasons. Among the possible causes for such behavior could be that the c -axis lattice parameter has decreased to the point where the (normally weakly coupled) BiO₂ layers have become more strongly bound, thereby closing the pathways for diffusion. Earlier work on pure Bi2212 has clearly demonstrated a significant depreciation in c parameter with oxygen uptake.² The c -axis data listed in Table I and elsewhere¹¹ show an analogous decrease in c upon Pb substitution in support of this possibility. In a related way, the substitution of Pb to the Bi site may fill the interstitial oxygen sites, preventing intercalation. The relaxation of the superlattice modulation may further exert a concomitant impact on the interstitial sites.

V. RAMAN SCATTERING

The phonons present in the Raman scattering spectrum have been identified as the motion of particular atoms within the Bi2212 structure.¹⁵ Thus, for the Pb-substituted crystals, we can compare the frequencies of these modes with those in the pure Bi2212 in order to discern the local effects of Pb. Figure 6 plots the $T=300$ K Raman scattering spectra of both Pb-substituted and pure Bi2212 single crystals. The spectra were measured with a triple spectrometer (at a resolution of 3 cm^{-1}) and collected by a nitrogen cooled charge-coupled device array. The $\lambda = 514 \text{ nm}$ line of an Ar⁺ laser was used for excitation. For each measurement, the samples were aligned so that both the incident and scattered light were polarized along the a axis of the crystal, defined as $Z(XX)\bar{Z}$ geometry, hereafter denoted by XX. The laser spot was focussed to a line, with typical dimensions of roughly $0.5 \times 0.05 \text{ mm}$, indicating that a considerably larger sample area is being probed than is the case for TEM or EDX. On this length scale, it was possible in some samples to see evidence of twinning, observed as an insensitivity of the polarized Raman spectrum to crystal rotation about the c axis. An example is shown in Fig. 7(b). The measured phonon spectra resemble a mix of XX and YY polarizations, independent of crystal orientation. Our result confirms similar observations of twinning made in Pb-substituted Bi2212.^{9,16}

The results of fits to the centers of each phonon peak are shown in Fig. 6. The most pronounced effect of Pb substitution is on the sharp mode at 118 cm^{-1} in the pure crystal,

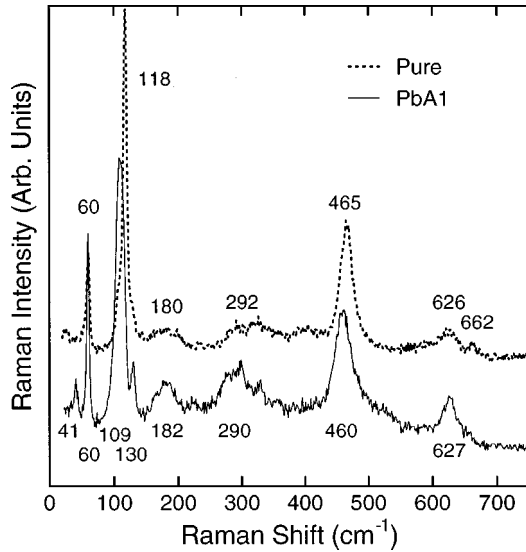


FIG. 6. The $T=300$ K Raman-scattering spectra of both Pb-substituted and pure Bi2212 single crystals in $Z(\overline{XX})\overline{Z}$ polarization.

which softens to 109 cm^{-1} . The identification of this mode remains controversial. Some researchers have identified it as the A_{1g} out-of-plane motion of the Bi atom,¹⁵ while others have suggested that it is more likely to be the A_{1g} out-of-plane motion of the Sr atom.^{13,16} The softening of this mode with Pb substitution has been used to argue for the latter, by suggesting that some of the Pb is substituting at the Sr site.

Roughly speaking, the frequency of a phonon is given by $\omega_{\text{ph}} \propto \sqrt{k/m}$, where m is the mass of the vibrating atom and k the local “spring constant.” Such a spring constant is proportional to the strength of local bonds, and inversely proportional to the distance from neighboring atoms in the lat-

tice. Thus, for a phonon to “soften” (go down in frequency), as the 118 cm^{-1} mode does, either k must decrease or m must increase. It has been argued^{13,16} that since Pb and Bi have similar masses, substituting Pb on the Bi site will have a negligible effect on ω_{ph} , and that therefore some of the Pb must be substituting for the much lighter Sr atoms. Further support for this argument is based on the fact that the lattice spacing (as indicated by the x-ray data in Table I) is decreasing with Pb substitution, along both the a and c directions, making a decrease in k unlikely. Furthermore, Regi *et al.*¹⁷ observed that Pb substitution precipitated an additional covalent bonding between adjacent BiO_2 layers. This further indicates that the primary effect of Pb substitution on the phonon frequency of a Bi mode should be an increase or “stiffening.” Therefore, the softening of the 118 cm^{-1} mode suggests an association with the Sr site and is indicative of at least a partial substitution of Pb for Sr.

Because the motion of the A_{1g} vibrations is primarily out of the a - b plane, the increased coupling related to a shorter crystal c -axis parameter should lead to stiffening for most of these phonons. However, it should be noted that most of the other A_{1g} phonons (all of those in Fig. 6) show little or no effect of Pb substitution. Possible exceptions include the c -axis vibration of the O atom in the SrO_2 layers, which softens from 465 to 460 cm^{-1} (consistent with Pb substitution for Sr), and the a -axis vibration of the O atom in the BiO_2 layer, which also softens from 292 to 290 cm^{-1} upon substitution of Pb. However, the behavior of the 292 cm^{-1} peak is highly sensitive to the alignment of the polarized light along the a axis, which may not be precise in the PbA1 spectrum. In particular, the increased strengths of the modes at 41 , 182 , and 292 cm^{-1} are likely due to leakage from the YY polarization.

Several other differences between the pure and Pb-substituted spectra are noticeable. The shift of the 118 cm^{-1} mode to 109 cm^{-1} allows the Cu c -axis A_{1g} vibration at 130 cm^{-1} to be fully resolved in XX polarization, but its frequency has not shifted measurably from that in the pure crystal. Finally, the small mode at 662 cm^{-1} , which has been identified as associated with the excess oxygen in the BiO_2 layers,^{15,18} has virtually disappeared upon Pb substitution. This confirms an earlier observation,¹⁶ and suggests that cation substitution at the Bi site relaxes the local conditions which made this mode Raman allowed. The disappearance of this mode may also be taken as evidence that the intercalated oxygen content is reduced with Pb substitution.

The low-temperature Raman spectra of two different Pb-substituted samples are presented in Fig. 7. The superconducting transition temperatures for each crystal are shown in the figure. Spectra are presented in both XX (A_{1g}) and XY (B_{1g}) polarizations (symmetries). Due to constraints on sample heating, the laser power is lower than that used in Fig. 6. The spectral resolution is set at 9 cm^{-1} in both polarizations. The raw intensities have not been scaled by the thermal Bose factor.

Solid lines represent data taken in the normal state, while the dashed lines plot the superconducting state spectra for each sample and polarization. In each case the effect of superconductivity is a depletion of scattering intensities at low frequencies accompanied by a peak in the range of 400 cm^{-1} . Such behavior has been attributed to the opening of a

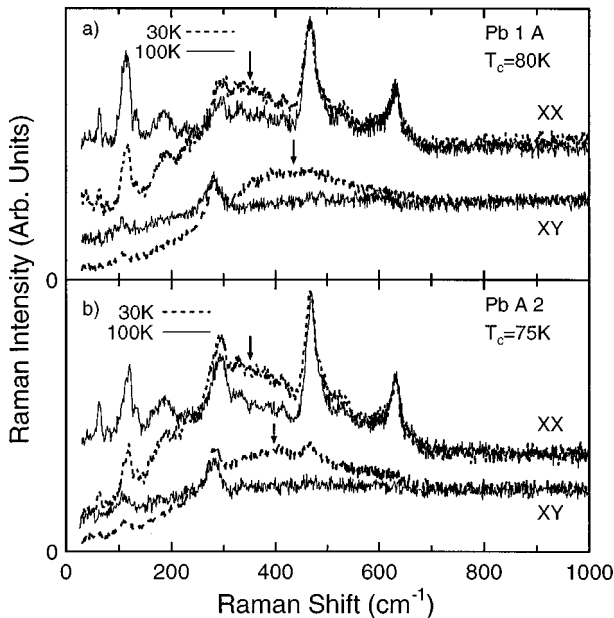


FIG. 7. The low-temperature Raman-scattering intensity of two different Pb-substituted Bi2212 crystals. Spectra are presented in both XX (A_{1g}) and XY (B_{1g}) polarizations (symmetries). Solid lines represent the normal state ($T=100$ K); dashed lines plot the superconducting state spectra ($T=30$ K).

superconducting energy gap at 2Δ in the electronic continuum below T_c . The observation of 2Δ peaks at different energies in different polarizations has been interpreted in terms of an anisotropic order parameter in the cuprates.¹⁹ The energies of the peaks are a sensitive function of doping level in Bi2212 with varying oxygen concentration.^{5,6} In the highly overdoped regime ($T_c < 70$ K), the peaks coalesce and move together toward lower energies. The Pb-substituted crystals in Fig. 7 are still in the “optimal” doping regime (but slightly overdoped) where the XY peak drops sharply with doping, while the XX peak remains relatively fixed.

This phenomenon is evident in a comparison of Figs. 7(a) and 7(b). At 30 K, the XY spectrum of the sample with $T_c=80$ K [Fig. 7(a)] crosses the 100 K spectrum at roughly 300 cm^{-1} and peaks at 440 cm^{-1} . By comparison, the crystal with $T_c=75$ K [Fig. 7(b)] shows the 30 K XY data crossing the 100 K spectrum at 260 cm^{-1} and peaking at 400 cm^{-1} . Thus the XY peak energy decreases more than the change in T_c ($440/400\text{ cm}^{-1} > 80/75\text{ K}$), while the XX peak energy remains fixed at roughly 350 cm^{-1} . Comparing the Raman spectra of these crystals with respect to pure samples postannealed in oxygen⁶ places them on the overdoped side of the maximum T_c , providing further indication of the doping properties of Pb^{2+} in Bi2212.

VI. CONCLUSIONS

Pb-substituted $\text{Bi}_2\text{Sr}_2\text{CaCu}_2\text{O}_{8+\delta}$ crystals have been grown and characterized using compositional, structural, magnetic, and optical techniques. The present results demonstrate that the sum of $[\text{Bi}]+[\text{Pb}]$ concentrations remains fairly constant, indicating that Pb primarily substitutes for Bi. However, the softening of the $118\text{ cm}^{-1} A_{1g}$ Raman-active phonon mode with substitution suggests that some fraction of the Pb also goes to Sr lattice sites. Overall, the basic orthorhombic crystal structure is preserved, but the superlattice modulation along b increases with Pb substitution. Both x-ray diffraction and Raman scattering show evidence of a - b plane twinning in some samples. The a and c lattice parameters decrease measurably with Pb substitution, providing a possible explanation for the relative difficulty in intercalating excess oxygen. Finally, the low-temperature Raman spectra reveal superconducting gap features which, when compared with pure samples annealed in various oxygen atmospheres, indicate that Pb substitution leads to cation overdoping.

ACKNOWLEDGMENTS

We wish to acknowledge the help of D. N. Dunn and M. Twigg with the TEM measurements. This work was supported by the Office of Naval Research.

-
- ¹C. Kendziora, L. Forro, D. Mandrus, J. Hartge, P. Stephens, L. Mihaly, R. Reeder, D. Moecher, M. Rivers, and S. Sutton, *Phys. Rev. B* **45**, 13 025 (1992).
- ²C. Kendziora, E. Skelton, R. J. Kelley, and M. Onellion, *Physica C* **257**, 74 (1996).
- ³Y. Kubo, Y. Shimakawa, T. Manako, and H. Igarashi, *Phys. Rev. B* **43**, 7875 (1991).
- ⁴M. Suzuki, *Phys. Rev. B* **39**, 2312 (1989).
- ⁵C. Kendziora, R. J. Kelley, and M. Onellion, *Phys. Rev. Lett.* **77**, 727 (1996).
- ⁶C. Kendziora and A. Rosenberg, *Phys. Rev. B* **52**, R9867 (1995).
- ⁷G. Blumberg, M. Kang, P. Abbamonte, M. V. Klein, M. Karlow, S. L. Cooper, and N. Kolesnikov, *Physica C* **235-240**, 1137 (1994); Moonsoo Kang, G. Blumberg, M. V. Klein, and N. N. Kolesnikov, *Phys. Rev. Lett.* **77**, 4434 (1996).
- ⁸J. Schneck, L. Pierre, J. C. Toledano, and C. Daguét, *Phys. Rev. B* **39**, 9624 (1989).
- ⁹Jian Ma, P. Almeras, R. J. Kelley, H. Berger, G. Margaritondo, X. Y. Cai, Y. Feng, and M. Onellion, *Phys. Rev. B* **51**, 9271 (1995).
- ¹⁰P. Fournier, A. Kapitulnik, and A. F. Marshall, *Physica C* **257**, 291 (1996).
- ¹¹L. Winkeler, S. Sadewasser, B. Beschoten, H. Frank, F. Nourvetne, and G. Guntherodt, *Physica C* **265**, 194 (1996).
- ¹²Rika Sekine, Yasuhiro Murakoshi, Shousuki Teratani, and Maki Kawai *Physica C* **246**, 385 (1995).
- ¹³K. C. Hewitt, X. K. Chen, X. Meng-Burany, A. E. Curzon, and J. C. Irwin, *Physica C* **251**, 192 (1995).
- ¹⁴C. Kendziora, Michael C. Martin, J. Hartge, L. Mihaly, and L. Forro, *Phys. Rev. B* **48**, 3531 (1993).
- ¹⁵Ran Liu, M. V. Klein, P. D. Han, and D. A. Payne, *Phys. Rev. B* **45**, 7392 (1992).
- ¹⁶J. Sapiel, J. Schneck, J. F. Scott, J. C. Toledano, L. Pierre, J. Chavignon, C. Daguét, J. P. Chaminade, and H. Boyer, *Phys. Rev. B* **43**, 6259 (1991).
- ¹⁷F. X. Regi, J. Schneck, H. Savary, R. Mellet, and C. Daguét, *Appl. Supercond.* **1**, 627 (1993).
- ¹⁸The authors of Ref. 16 associated the 650 cm^{-1} mode with the $\text{Bi}_2\text{Sr}_2\text{CuO}_{6+\delta}$ (Bi2201) “impurity” phase and argued that its disappearance indicated that Pb stabilized growth of the Bi2212 structure.
- ¹⁹T. P. Devereaux, D. Einzel, B. Stadlober, R. Hackl, D. H. Leach, and J. J. Neumeier, *Phys. Rev. Lett.* **72**, 396 (1994).